

Optimizing Wireless Discontinuous Reception via MAC Signaling Learning

Adriano Pastore¹, Senior Member, IEEE, Adrián Agustín de Dios¹, Senior Member, IEEE, Álvaro Valcarce², Senior Member, IEEE

¹Centre Tecnològic de Telecomunicacions de Catalunya (CTTC), Av. Carl Friedrich Gauss 7, 08860 Castelldefels, Spain

²Nokia Networks France, 12 Rue Jean Bart, 91300 Massy, France

Corresponding author: Adriano Pastore (email: adriano.pastore@cttc.cat).

This work has been funded by Nokia through its program of academic partnerships.

ABSTRACT We present a Reinforcement Learning (RL) approach to the problem of controlling the Discontinuous Reception (DRX) policy from a Base Transceiver Station (BTS) in a cellular network. We do so by means of optimally timing the transmission of fast Layer-2 signaling messages (a.k.a. Medium Access Layer (MAC) Control Elements (CEs) as specified in 5G New Radio). Unlike more conventional approaches to DRX optimization, which rely on fine-tuning the values of DRX timers, we assess the gains that can be obtained solely by means of this MAC CE signalling. For the simulation part, we concentrate on traffic types typically encountered in Extended Reality (XR) applications, where the need for battery drain minimization and overheating mitigation are particularly pressing. Both 3GPP 5G New Radio (5G NR) compliant and non-compliant (“beyond 5G”) MAC CEs are considered. Our simulation results show that our proposed technique strikes an improved trade-off between latency and energy savings as compared to conventional timer-based approaches that are characteristic of most current implementations. Specifically, our RL-based policy can nearly halve the active time for a single User Equipment (UE) with respect to a naïve MAC CE transmission policy, and still achieve near 20% active time reduction for 9 simultaneously served UEs.

INDEX TERMS 5G New Radio, Deep Reinforcement Learning, Discontinuous Reception (DRX), Energy Efficiency, MAC protocol learning.

I. INTRODUCTION

THE MAC layer protocol specifications up to Fifth Generation (5G) networks, as well as all earlier predecessor standards such as Long Term Evolution (LTE), have been engineered by hand, mostly following expert guidelines and heuristics. As a promising alternative, recent advances in Multi-Agent Reinforcement Learning (MARL) have opened up new possibilities for an experience-driven approach to protocol design [1].

Specifically, in this work, we apply a MARL approach to the design of the DRX control policy. DRX is a network function that lets UEs switch intermittently between an active and an inactive (a.k.a. sleep) state. During the inactive state, UEs cease to monitor and decode the Physical Downlink Control Channel (PDCCH), thus saving some energy in the process. However, this comes at the cost of increased end-to-end latency and a lower Channel State Information (CSI) quality due to missed opportunities for channel reporting.

DRX is an important technique for reducing battery drain in mobile devices, as well as for improving the energy

efficiency of 5G radio links. In fact, power-saving efforts in 5G communications (and beyond) are crucial, since energy efficiency is a requirement that transversally impacts all use cases (eMBB, mMTC, URLLC) [2]. As highlighted in [3], PDCCH monitoring is a primary contributor to UE power consumption [4]. In fact, for common traffic types, the overhead due to PDCCH activity is disproportionately large compared to the energy expended on payload data via the Physical Downlink Shared Channel (PDSCH). For instance, according to [3, Fig. 8], under an FTP-3 traffic model, the time during which the UE *solely* processes the PDCCH accounts for 92% of the total power consumption, while time spent processing the PDSCH only contributes 6% (with the remaining 2% representing sleep). This asymmetry is largely due to the *blind decoding* process that UEs perform to obtain the PDCCH. In addition, unlike at the BTS, energy inefficiencies have multifaceted impacts on the UE performance and the comfort of the human user. This is mostly due to the prevalence of battery-powered devices, heating effects, etc. Optimizing DRX performance is, therefore, a key

priority for Mobile Network Operators (MNOs) to ensure that the UEs have enough battery to get through the day.

Most attempts at DRX optimization have focused on finding the best values for the set of timers that steer the 5G DRX function. These are namely the *drx-InactivityTimer*, the *drx-onDurationTimer*, and the *drx-onDuration* parameter (see [5] for details on these). More recently, signaling-based approaches, such as *Search Space Set Group (SSSG) switching* and *PDCCH skipping* were standardized in 3rd Generation Partnership Project (3GPP) Rel-17, as described in [6]. However, usage of these is yet to reach live networks, mainly due to difficulties in finding a logic to steer them. Fortunately, the abundance of data that can be obtained in cellular networks paves the way for Machine Learning (ML) approaches to this problem. Authors in [7] and [8], for example, train traffic predictors and then derive the timer values from the obtained forecasts. On the other hand, [9] proposes a contextual bandit and non-standard 5G signaling to select among a set of predefined DRX configurations.

Given the inherent difficulties in producing truly general traffic forecasts, and our practical wish to remain within 5G-compliant signaling, we set off to optimizing DRX exclusively using the tools available in today's cellular networks. A potential approach to this could be to treat the optimization of DRX timers as a black-box optimization problem. However, 5G networks only permit updating the value of these timers via Layer 3 signaling, which requires slow and heavy RRC reconfigurations. This is not flexible or fast enough to leverage the energy-saving opportunities that modern lightweight devices require. For these reasons, we decided to exploit some underused L2 signaling opportunities. To this end, we devised a RL approach compatible with 5G NR specifications such as those in recent releases of 3GPP Technical Specification (TS) 38.321, and compare it to the state-of-the-art baselines specified in those standards. To the best of our knowledge, this is the first reported usage of ML to enhance UE power savings via low-layer signaling.

Specifically, these baselines are rule-based policies that rely on a timers-based logic. This logic, described in Section A, controls a collection of timers that will count down and be reset depending on traffic demands. The timer logic is replicated at both ends of the BTS-UEs links, to guarantee BTS and UEs timers synchronization.

Alternatively to this timers-based logic, the *start* of an inactive phase may also be triggered by the BTS via the transmission of a dedicated MAC CE. The *termination* of inactive phases, in turn, is still dictated by time-out events. This intervention of the BTS via CE transmissions prompts an inactivity timer to be reset and thus partly overrides the “fallback” logic of timers. These CEs are standardized, but their usage is not widespread in commercial implementations. Our simulations suggest that BTS-side RL policies for timing the transmission of CEs can be used effectively to improve the DRX-induced power savings under stringent latency requirements.

II. SYSTEM MODEL

We consider a downlink setting involving one BTS and one or more UEs, as sketched in Figure 1.

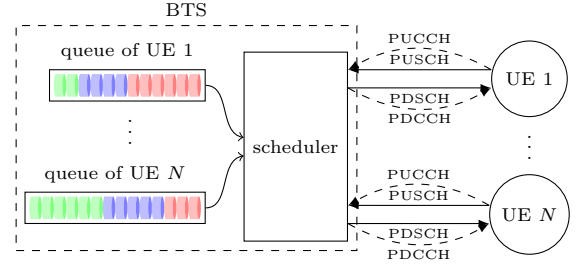


FIGURE 1. Wireless network architecture.

The UE queues store a collection of Radio Link Control (RLC) Protocol Data Units (PDUs) that are assembled into MAC Service Data Units (SDUs), or so-called Transport Blocks (TBs). We assume that one TB at most can be transmitted by the BTS in each Transmission Time Interval (TTI), and that the TTI duration remains fixed to 1 millisecond throughout. The UEs can communicate with the BTS through an error-free control channel, Physical Uplink Control Channel (PUCCH), allowing to acknowledge or not the received TB. The scheduler is responsible for assigning the radio resources to the UEs taking into account which UEs have information in their respective downlink queues and which ones are active, listening to the PDCCH. We assume that the scheduler is given, for example, based on Round Robin, and we cannot modify its policy. Every time the scheduler takes a decision, it informs the respective UE through the PDCCH.

At each UE, we distinguish the following states:

- If $W_u(t) = 1$ (active), the u -th UE tries to decode the PDCCH in TTI t to elucidate if a TB is transmitted in the PDSCH.
- If $W_u(t) = 0$ (inactive), the u -th UE does not try to decode the PDCCH in TTI t . This is the equivalent of a sleep or energy-savings state at the UE.

A. DRX policy based on timers

In 3GPP 5G NR, inactive period durations are determined by timers, providing the BTS with precise knowledge of each UE's status for scheduling considerations. 3GPP defines the following parameters to configure the timers:

- **DRXCycle**. The total duration during which a UE's DRX timer is valid (active and inactive periods).
- **onDurationTimer**. The part of the *DRXCycle* during which the UE is active.
- **drx-onInactivityTimer**. This timer keeps the UE active after receiving a message. Upon message reception, the timer is reset. Once it expires, the UE transitions to an inactive state until the current DRX cycle concludes.

The general working principle, with some simplifications, is best illustrated by Figure 2. We assume that the UE is actively monitoring the PDCCH and receiving downlink data. Then, at some point, this UE's downlink buffer is depleted, and the scheduler ceases to notify the UE about new data. The UE continues to monitor the PDCCH during a number of consecutive TTIs denoted by **drx-onInactivityTime**. When the inactivity timer expires (i.e., it counts down to zero), the UE switches to a periodic behavior that alternates between short listening periods ("ON duration" defined by **onDurationTimer**) and prolonged inactivity periods ("DRX sleep" in Figure 2) that end at each start of a new DRX cycle.

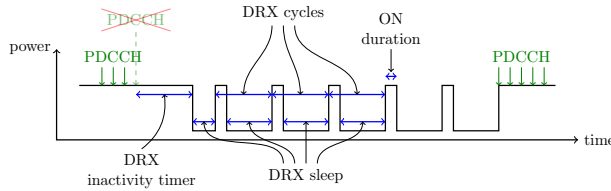


FIGURE 2. Power consumption profile over time for a UE operated with timer-based DRX.

B. Traffic model and L2 queue management

At the BTS, a stochastic process governs the arrival of user data to the MAC as a sequence of RLC PDUs (cf. Figure 3). In simulations, we have modeled this arrival process to mimic Extended Reality (XR) traffic, which is representative of augmented reality and cloud gaming use cases. Such type of traffic is well known to have extreme throughput and latency requirements. Furthermore, reducing the power consumption of wearable devices such as Virtual Reality (VR) headsets is essential to mitigate user discomfort for overheating reasons. Minimizing battery drain is also a highly relevant target [10], [11].

TABLE 1. XR traffic model as described in [11].

| | |
|----------------------|--|
| Interarrival time: | 16.6 ms (corresponds to 60 frames per second) |
| Average data rate: | 60 Mbit/s |
| Average packet size: | 1 Mbit (equals data rate/fps) |
| Packet size: | truncated Gaussian with: standard dev. = 10.5% of the mean Min = 50% of the mean Max = 150% of the mean |
| Jitter: | truncated Gaussian with standard dev. = 2 ms Min = 4 ms Max = 4 ms |

For these reasons, XR traffic is an ideal traffic type to study the performance of DRX solutions. A thoroughly validated mathematical model of XR traffic has been proposed

in [11] and is summarized in Table 1. In contrast to other well-known models like FTP3 traffic, the XR traffic pattern is of quasi-periodic nature (interarrival times have low variance, and stay stable up to jitter effects), which gives this traffic type a certain level of predictability and as a consequence, substantial potential for DRX-managed power savings.

We follow a standard 5G NR stacked architecture, where downlink RLC PDUs are handled as SDUs by the MAC layer. These are accumulated in a separate queue for each user. The MAC layer may then assemble multiple single-UE SDUs into a single TBs (with possible insertion of MAC CEs). The TB size is selected to be commensurate with the channel conditions informed by the Physical Layer (PHY) layer (cf. Subsection D).¹ The TBs are then conveyed from the BTS PHY to the UE via the PDSCH, and MAC SDUs are deleted from the queue only after the BTS receives a corresponding Acknowledgement (ACK) message from the UE via the PUCCH.

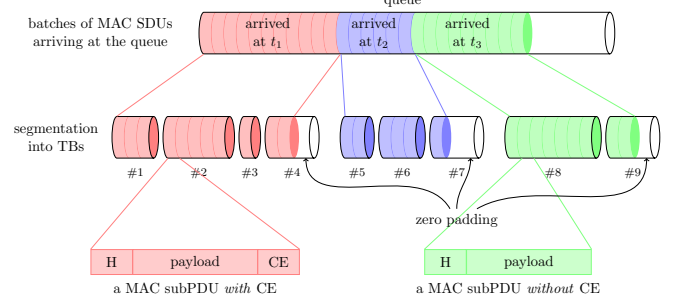


FIGURE 3. Illustration of the TB generation. In this example, the queue contents are collections of MAC SDUs that have arrived at TTIs t_1 , t_2 and t_3 , respectively. They get segmented by the MAC layer into a sequence of TBs of different sizes (depending on the channel conditions). Zero padding is applied to fill out the last TB corresponding to each batch of payload data.

The CEs are reserved fields that can be appended to any single MAC subPDU (cf. Figure 3). We distinguish between legacy CEs (that are part of the 5G NR technical specifications) and new, additional CEs whose semantics we may customize to our needs. The 3GPP standard defines two legacy CEs:

- **DRX_command_MAC_CE** (Logical Channel ID (LCID) 60) instructs the UE to finish the current active time and enter into a short DRX cycle.
- **Long_DRX_command_MAC_CE** (LCID 59) instructs the UE to finish the current active time and start a long DRX cycle.

For simplicity, we consider only the CE with LCID 59, i.e., we restrict ourselves to long DRX cycles. Note that these CEs partly override the timer logic, in the sense that they command the UE to enter inactive mode immediately, instead

¹For simplicity, we will assume that the size of batches of MAC SDUs entering the queue, as well as the size of TBs, are arbitrary integer-valued (in bits).

of waiting for a timeout of the DRX inactivity timer, as in conventional timers-based DRX.

C. Performance indicators

We will focus on two Key Performance Indicators (KPIs), namely *activity* and *latency*. The former is a proxy to the power consumption of a UE and we define it as the average fraction of time that the u -th UE has been active during a window of T TTIs:

$$\langle W_u \rangle = \frac{1}{T} \sum_{t=1}^T W_u(t). \quad (1)$$

The latter is evaluated as an average SDU delay as follows: Let $D_u^{(i)}$ denote the delay of the i -th downlink SDU for user u , that is, the number of TTIs that have elapsed between the arrival of the i -th SDU in the u -th queue, and its successful delivery at the corresponding UE.² If a total of S_u SDUs are transmitted to the u -th UE in the run of an experiment, then the average SDU latency experienced by the u -th UE is defined as

$$\langle D_u \rangle = \frac{1}{S_u} \sum_{i=1}^{S_u} D_u^{(i)}. \quad (2)$$

For practical reasons, we focus on constraining the delay of a statistically significant fraction of all SDUs. For instance, we may require that the fraction

$$\sigma_u = \frac{|\{i: D_u^{(i)} \leq \Delta\}|}{S_u} \quad (3)$$

of SDUs that satisfy some maximum target latency of Δ be larger than some threshold β (i.e., $\sigma_u \geq \beta$). We denote this quantity as **user satisfaction**. For these activity and latency metrics to be realistic and free of exogenous artifacts, the packet arrival rate needs to be low enough so as to ensure that all queues remain stable, in the sense that the queue length is a stationary process. In simulations, we have tested this stability empirically, by verifying that queue lengths did not grow unbounded (leading to buffer saturation) for long runs of experiments.

D. Modeling the PHY layer

Each TB that is conveyed from the BTS to an active UE at time t has a certain probability $\epsilon(t)$ of being received incorrectly, which fluctuates over time depending on the channel conditions and channel estimation quality.

To define the stochastic process $\epsilon(t)$ we first adopt a simple first-order autoregressive fading model for the downlink channel gain $h(t)$, i.e.,

$$h(t) = \rho h(t-1) + \sqrt{1-\rho^2} w(t) \quad (4)$$

²For example, in Figure 3, supposing that the SDU #5 is contained in TB #2 (colored in red), then its delay $D_u^{(5)}$ is the difference between the moment (i.e., TTI index) at which TB #2 is received at the UE, and the moment at which SDU #5 has entered the queue (which in this example is t_1).

with parameter $\rho \in (0, 1)$, where the white noise $w(t) \sim \mathcal{CN}(0, 1)$ follows an independent complex normal distribution. Inspired by the Jakes-Clarke one-ring model, the fading cross-correlation ρ between two consecutive TTIs can be expressed as (cf. [12, Eq. (4)])³

$$\rho = J_0(2\pi f_D T) \quad (5)$$

where $J_0(x) = \frac{1}{2\pi} \int_{-\pi}^{\pi} e^{jx \sin(t)} dt$ denotes the Bessel function of the first kind of order zero, T stands for the TTI duration (one millisecond), $f_D = f_c v/c$ stands for the maximum Doppler spread, f_c for the carrier frequency, v for the UE's velocity and c for the speed of light.

The UEs are assumed to be cognizant of the exact channel coefficient $h(t)$ at any time t , but report the current value of $h(t)$ only *periodically* back to the BTS over the PUCCH. Whenever a UE is in the DRX inactive state in a time slot wherein a CSI report is due, said report is skipped, as illustrated in Figure 4. A similar approach can be found in [12].

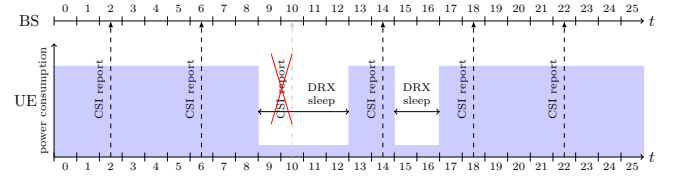


FIGURE 4. Pattern of periodic CSI reporting with interruptions due to the DRX inactive mode.

III. FORMULATION AS A PROTOCOL LEARNING PROBLEM

The interaction between the BTS and UEs through CEs appended to TBs forms a time-discrete, sequential decision-making process. This process, governed by a *policy*, is optimized using RL at the BTS. Specifically, at each TTI, the agent decides which MAC CE (if any) to send to each UE, making independent decisions for each UE (e.g., for 10 connected UEs, 10 independent decisions are made). Given the small action space, we use a value-based RL algorithm, namely Deep Q-Network (DQN) [13]. While UE-specific models are possible, a single agent model is more practical if it generalizes well across different UEs. To ensure that the agent can generalize well across UEs with different traffic patterns and channel conditions, the state space includes UE-specific features (e.g., queue length, age of packets in the queue) and cell-specific features (e.g., number of active UEs, total queue length). Thus, we trained a single DQN agent with data from all UEs. This strengthens the agent's generalization ability, allowing it to make DRX signaling decisions based on each UE's local context. The DQN is

³Note that this is not an exact application of the Jakes-Clarke model, since the latter describes a fading autocorrelation function described by $E[h(t)h(t-\Delta t)^*] = J_0(2\pi f_D \Delta t)$. We limit ourselves to applying this expression of the autocorrelation function to a single TTI slot.

updated based on the observed UE traffic, enabling it to adapt to different traffic types and channel conditions for each UE. In the following, we define the Markovian state and action spaces available to the RL agent at the BTS.

A. State vector definition

We consider the following UE-specific features to be available to the RL agent as part of the state vector at time t :

- **Acknowledgment:** a binary variable indicating whether or not the downlink TB transmitted at time $t - D_{\text{HARQ}}$ was received correctly. We assume for simplicity that this acknowledgment arrives *before* the BTS policy execution at time t . The acknowledgment is therefore taken into account for computing the BTS action at time t (see Section C). D_{HARQ} denotes the Stop-And-Wait (SAW) Hybrid ARQ (HARQ) process delay, which for simplicity in our simulations we set to $D_{\text{HARQ}} = 1$.
- **Scheduling indicator:** a binary variable indicating whether the UE is scheduled for transmission at time t .
- **Time until next DRX long cycle:** a natural number that counts down the number of TTIs remaining until the start of the next DRX long cycle.
- **Age of packets in queue:** the number of TTIs that have elapsed since the oldest RLC PDU entered the downlink queue.
- **Queue length:** the traffic volume (in number of bits) of the downlink queue for UE u .
- **Remaining time in current DRX state:** the number of remaining TTIs until the timers-based policy would trigger a DRX state change.
- **Resource usage:** a categorical variable with possible values in $\{0, 1, 2, 3\}$ indicating how the radio resources were used in the previous step:
 - 0: the UE u was scheduled and successfully transmitted a TB containing at least one MAC subPDU with payload.
 - 1: the UE u was scheduled and successfully transmitted a TB containing one or more MAC subPDUs. None of them contained payload.
 - 2: the UE u was scheduled, but the TB transmission failed.
 - 3: the UE u was not scheduled.

In addition to these UE-specific features, the following cell-specific features are also available to the RL agent:

- **Number of active UEs:** this indicates how many UEs are in DRX active state in the current time step.
- **Total queue length:** the total number of bits at the queues of all active UEs combined.

We collectively denote a vector containing all these features as $S_u(t)$. As can be seen from the above listing, there are eight numerical features and one quaternary categorical feature (resource usage). The latter being one-hot encoded

in the neural implementation of the RL policy, this results in $S_u(t)$ being represented by 12 inputs.

B. Reward function

The reward function is designed to minimize UE activity (modeled through the signal $W_u(t)$) while maintaining a minimum latency satisfaction $\sigma_u(t)$. In our experiments, we strive to achieve that a target fraction β of SDUs meets a given target maximum latency Δ . For this purpose, at any time t we look back at a fixed number $N = 20$ of the most recently transmitted SDUs and compute the metric σ_u based on (3) over that sample. We then define the reward function $R_u(t)$ of the u -th UE as the “satisfaction gap” $\sigma_u(t) - \beta$ whenever $\sigma_u(t) < \beta$. Otherwise, the reward function is equal to the sleep state indicator $1 - W_u(t)$. That is,

$$R_u(t) = \begin{cases} \sigma_u(t) - \beta & \text{if } \sigma_u(t) < \beta \\ 1 - W_u(t) & \text{if } \sigma_u(t) \geq \beta \end{cases}$$

We further define the average *cumulative reward* per UE as the sum of reward values accumulated over the course of an episode, averaged over the set of active UEs, of which there is a fixed number $U \in \{1, \dots, 9\}$ in any given episode, i.e., $\frac{1}{U} \sum_{u=1}^U \sum_{t=1}^{N_t} R_u(t)$.

C. Actions

The definition of the action space for the RL agent depends on whether we are training in a 5G NR-compliant scenario or not. As detailed in Section IV below, we consider two cases, with respective action space sizes $|\mathcal{A}| = 2$ (compatible with pre Rel-17 5G NR) and $|\mathcal{A}| = 7$ (compatible with Rel-17 5G NR and beyond):

- Case 1 ($|\mathcal{A}| = 2$):
 - If $A_u(t) = 1$: the BTS includes a Long_DRX_command_MAC_CE (LCID 59) in the first MAC SDU of the next TB. This commands the UE to start a long DRX inactivity period immediately.
 - If $A_u(t) = 0$: no MAC CE is included. Hence, the TB only contains a header and data payload.
- Case 2 ($|\mathcal{A}| = 7$): same as Case 1, except that the inactivity duration can be selected with more granularity via a custom CE. The value of $A_u(t) \in \{0, 2, 4, 6, 8, 10, 12\}$ denotes the duration of this inactivity as a number of TTIs. This is similar to the *PDCCHSkippingDurationList* recently introduced by 3GPP in Rel-17.

Note that, for simplicity of Case 1, we do not consider the usage of the Short DRX command, which is rarely used in practical deployments.

D. Experience Replay Memory (ERM) management

The transition tuples stored into the ERM are defined as $(S_u(t), A_u(t), R_u(t), S_u(t + 1))$, where $u \in \{1, \dots, U\}$.

Note that, in contrast to the textbook setting of single-agent RL, in our setting the BTS policy is not executed at *every* TTI index t , but only *conditionally* when the receiving UE is known to be active (listening). Otherwise, the UE is known to be inactive and no policy is executed. In the latter case (when the UE is inactive), we deviate from the classic DQN implementation as follows:

- We force the BTS policy to choose a null action (by hard-coding a switch).
- We do not store the corresponding transition into the ERM. This is for practical reasons due to the limited capacity of the ERM. Storing transitions containing the null action might overwrite other *more interesting* RL-guided transitions.

IV. EXPERIMENTAL VALIDATION

TABLE 2. System settings

| | |
|------------------------------------|------------------|
| TTI | 1 ms |
| Bandwidth | 100 MHz |
| Effective BW for DL payload | 72 MHz |
| Fading cross-correlation ρ | 0.99 |
| CSI update period T_{CSI} | 10 ms |
| Traffic type | XR (see Table 1) |
| Number of UEs | 1 to 9 |
| SNR | 10 dB |
| <i>drxInactivityTimer</i> | 8 ms |
| <i>drxOnDurationTimer</i> | 8 ms |
| <i>drxLongCycle</i> | 16 ms |

We assess the performance of the proposed RL-based MAC signaling DRX scheme in a system-level simulation where one BTS serves several UEs. Table 2 collects all configuration details, where the value of the *drxLongCycle* has been aligned with the packet interarrival time for XR traffic (other traffic types, such as non-GBR data might use values closer to 160 ms, voice might use 40 ms, etc.). Finally, we compare our method against the following baselines:

- 1) **Always ON:** UEs listen decode PDCCH on all TTIs.
- 2) **Timers-based:** the UEs DRX activity and inactivity periods are fully controlled via Radio Resource Control (RRC) timers as per 3GPP standards.
- 3) **Naïve policy:** in addition to RRC timers, the BTS also instructs UEs via legacy CEs (LCIDs) to commence inactive periods as soon as their traffic queue empties.
- 4) **Random policy:** in addition to the RRC timers, the BTS sends legacy CEs with probability $1/2$ each TTI.

These baselines were benchmarked against the following RL-based solutions:

- 1) **RL policy** ($|\mathcal{A}| = 2$): as in the timers-based baseline (item 2 above), but the BTS now decides whether or

TABLE 3. Reinforcement Learning hyperparameters

| | |
|--|--|
| ERM size M (number of transition tuples) | 10^5 |
| Batch size B (number of transition tuples) | 256 |
| Size $ \mathcal{A} $ of action space | 2 or 7 |
| Number of hidden layers | 1 |
| Neurons per hidden layer | 40 |
| Activation function (hidden layers) | rect. linear unit |
| Activation function (output layer) | softmax |
| Input layer size (for a history size of 3 TTIs) | $12 \times 3 = 36$ |
| Output layer size (equals action space size) | 2 or 7 |
| Loss function | Huber loss (param. 1) |
| Number of inferences between model updates | 100 |
| Number N of SDUs for computing metric σ_u | 20 |
| Discount factor γ | 1 |
| Learning rate LR | $10^{-2} \rightarrow 10^{-5}$ (tuning) 10^{-3} (training) |
| Number of indep. training sessions N_{runs} | 8 (tuning), 30 (training) |
| Number N_{ep} of episodes per run | 750 (training) 250 (evaluation) |
| Number N_t of time steps per episode | 8000 |
| Epsilon-greedy decay | $0.8 \rightarrow 10^{-6}$ |
| Delay stringency β | 0.95 |

not to send legacy 5G NR-compliant MAC CEs based on a RL policy.

- 2) **RL policy** ($|\mathcal{A}| = 7$): as in the previous RL scheme, but the BTS now decides to send custom CEs that instruct the UE to commence inactive periods of variable duration based on a RL policy (see Subsection C for details).

All UEs share the same XR traffic model and RRC timer configurations, with the DRX inactivity timer set to 8 ms following commercial products, and the DRX long cycle duration set to 16 ms for alignment with the XR packet interarrival time. The naïve, random and RL policies are always *stabilized* by a hard-coded rule that prohibits the transmission of any CE in case of queue saturation. This is a trivial fix to improve the performance of these policies, and it felt only fair to include it here.

A. Hyper-parameter tuning

Most of the hyper-parameter values we have selected are commonly used across the RL literature. However, we have opted for a slightly larger batch size B of 256 to reduce noise during gradient descent updates. In addition, we have also fine-tuned the learning rate and the discount factor by evaluating the performance of the proposed scheme across $N_{\text{runs}} = 30$ randomized training runs for each candidate hyper-parameter value. Then, we select the one yielding the highest average (over the training runs) cumulative reward. Each training run consists of $N_{\text{ep}} = 750$ independent

episodes with $N_t = 8000$ time steps each, where the first episodes are largely devoted to exploration. Specifically, the exploration–exploitation balance is controlled by a parameter $\epsilon \in [0, 1]$ which is exponentially decreased from 0.8 to 10^{-6} , in steps every 30 episodes, reaching its final value of 10^{-6} after 300 episodes, where it stops decaying.

Once the best configuration is selected, we carry out extensive training ($N_{\text{runs}} = 30$) to derive the RL model, selecting the one with the highest historic cumulative reward.

B. Simulation results

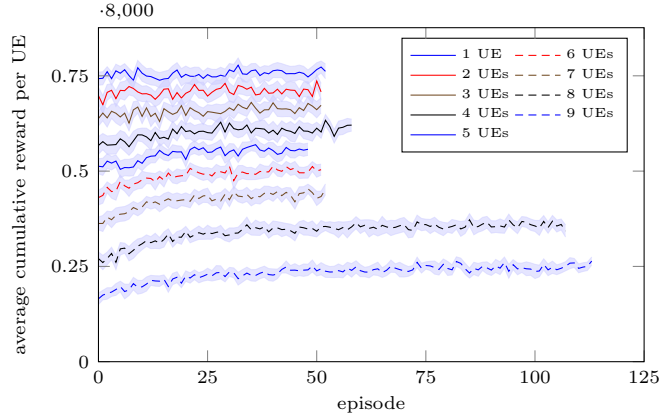


FIGURE 5. Convergence of the cumulative reward for $|\mathcal{A}| = 2$ and a variable number of UEs, averaged over $N_{\text{runs}} = 30$ independent runs of the training. Traffic statistics, system model and parameters are as described in Tables 1, 2, 3.

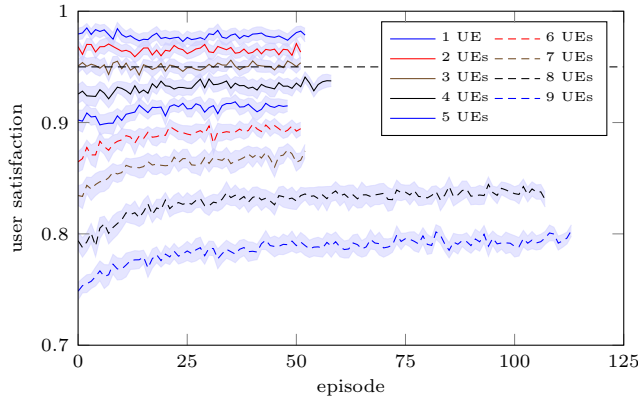


FIGURE 6. Convergence of the user satisfaction corresponding to the same training runs as in Figure 5.

In Figures 5 and 7, we show the convergence of the average cumulative reward per UE, as previously defined in Section B, for the cases $|\mathcal{A}| = 2$ and $|\mathcal{A}| = 7$, respectively. Note that the y axes indicate the cumulative reward per UE and per TTI, and the indication “ $\cdot 8,000$ ” at the axis top is a reminder that y -axis values need to be multiplied by the corresponding factor to obtain the cumulative reward per episode (since there are 8000 TTIs per episode, cf. Table 3). Each curve represents a mean value over $N_{\text{runs}} = 30$

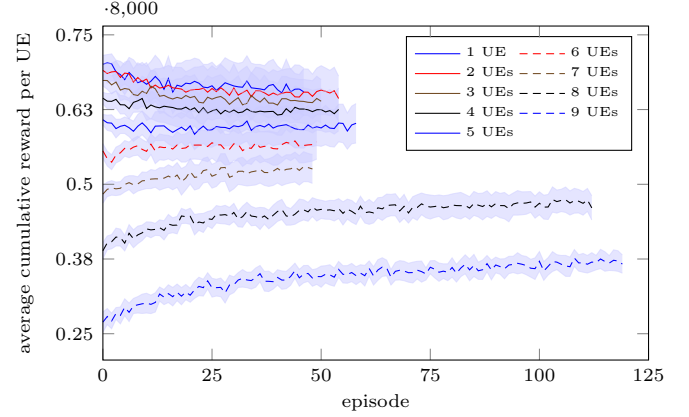


FIGURE 7. Convergence of the cumulative reward for $|\mathcal{A}| = 7$ and a variable number of UEs, averaged over $N_{\text{runs}} = 30$ independent runs of the training. Traffic statistics, system model and parameters are as described in Tables 1, 2, 3.

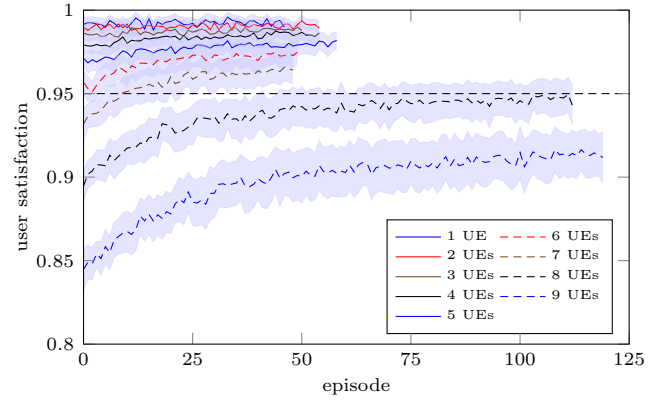


FIGURE 8. Convergence of the user satisfaction corresponding to the same training runs as in Figure 7.

independent training sessions, plotted along with a 95% t -student confidence interval. We intended to learn policies that are robust to variations in the number of UEs. To achieve this, we randomly varied (from 1 to 9) the number of active UEs between episodes in an i.i.d. fashion (with more weight given to scenarios with 8 and 9 UEs). The training curves in Figure 5 have been arranged separately based on the number of active UEs, offering a more distinct portrayal of trends. The randomness in the activation of UEs explains the different curve lengths visible in Figures 5 through 8. Figures 6 and 8 show the evolution of user satisfaction for the same training experiments as in Figures 5 and 7, respectively. The dashed line indicates the target delay threshold $\beta = 0.95$ that the user satisfaction should ideally exceed. We see that with the 5G NR compliant scheme ($|\mathcal{A}| = 2$) we can only serve up to 3 UEs with satisfactory delays, whereas the more granular signaling ($|\mathcal{A}| = 7$) allows to serve up to 8 UEs.

In Figure 9, we illustrate the average performance of the different baselines and trained policies in the activity–delay trade-off plane. Here, the x -axis denotes the SDU delay $D = \frac{1}{U} \sum_{u=1}^U D_u$ (in ms), and the boxplots depict the median,

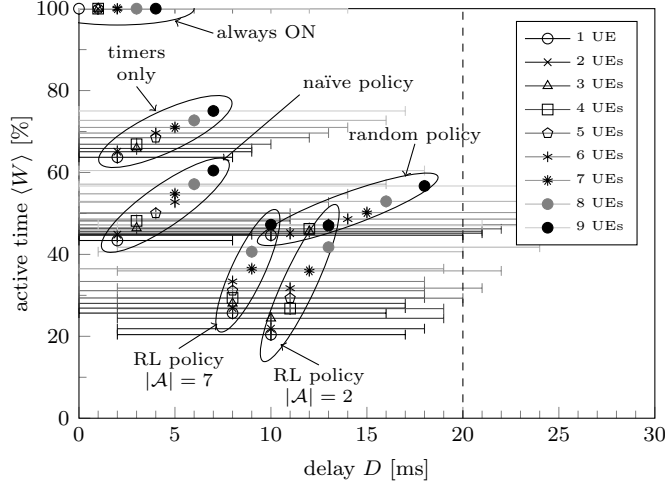


FIGURE 9. Tradeoff between average active time and delay quantiles for a varying number of UEs and different DRX schemes in comparison, with same parameters as in Figure 5. For every configuration, the average delay is shown at the marker position (see legend) together with a horizontal bar with right and left whiskers, which are placed at the 5-th and 95-th delay percentile, respectively.

and 5-th/95-th percentiles of the delay distribution for each solution. Similarly, the y -axis denotes the fraction of active time $\langle W \rangle = \frac{1}{U} \sum_{u=1}^U \langle W_u \rangle$ (as a percentage), where $U \in \{1, \dots, 9\}$ is the number of UEs. In this plot, we compare the performance of RL-based DRX for $|\mathcal{A}| = 2$ and $|\mathcal{A}| = 7$ against several baselines.

For each configuration, a horizontal boxplot shows the median (corresponding to the plot mark, as in the legend) as well as left and right whiskers that correspond to the 5-th and 95-th percentile of the empirical SDU delay distribution, respectively. The maximum admissible delay (20 ms) is displayed by a dashed vertical delimiting line. Ellipses are a visual help to distinguish clusters of boxplots that correspond to different configurations.

Note that the simulation results for the RL agents ($|\mathcal{A}| = 2$ and $|\mathcal{A}| = 7$) correspond to a single agent, respectively, which is exposed during training to an environment with a number of active UEs that varies randomly between 1 and 9 (as in the context of Figure 5), and which is then evaluated for a *fixed* number of active UEs (this value ranging from 1 to 9). The other schemes correspond to an Always ON operation (no DRX), timers only, as well as two baseline schemes: the naïve policy consists in having every UE send a CE as soon as its queue is empty. The random policy decides whether or not to send a CE based on a Bernoulli-0.5 variable (fair coin flip). Recall that the naïve, random and RL policies are always *stabilized* to prevent queue saturation, as explained at the beginning of Section IV.

We see that the RL-based CE-controlled DRX outperforms all baselines in terms of activity reduction (and thus also the DRX-related power savings) by a substantial margin, while meeting the 20ms latency target for most configurations: by keeping track of the locations of right whiskers on the

boxplots (95-th percentiles of SDU delay) in Figure 9, we see that up to 5 UEs can be served with satisfactory delays with a 5G NR compatible RL policy ($|\mathcal{A}| = 2$) whereas 8 UEs can be served with the more granular policy ($|\mathcal{A}| = 7$).

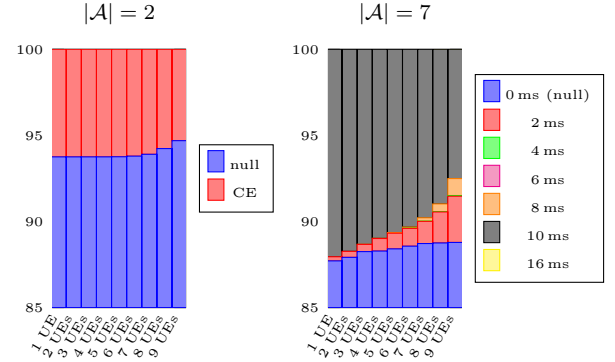


FIGURE 10. Relative frequencies (in percentages) of the selected actions.

Finally, Figure 10 shows the relative frequencies of selected actions. We observe that the null action (corresponding to 0 ms) is by far the most frequent action. We can also appreciate how a richer action space ($|\mathcal{A}| = 7$ instead of $|\mathcal{A}| = 2$) seems to be exploited by the RL agent by privileging certain actions over others. In our case, it is mostly those actions corresponding to 10 ms, 2 ms and 8 ms which are utilized with non-negligible probability. This is likely dependent on the specificities of the XR traffic pattern and some of our parameter choices, e.g., the value of 16 ms for the *drxLongCycle*.⁴

V. CONCLUSION

This paper has shown that a signaling approach to DRX can augment a 5G NR-compliant and timers-based conventional DRX scheme. We have also shown that RL techniques can discover deterministic DRX control policies that leverage MAC CEs to trigger additional inactivity periods with judicious timing. Simulation results have shown the potential of both CEs and RL to achieve substantial energy savings beyond timers-based DRX baselines while still fulfilling strict QoS latency requirements. This opens up the possibility of fine-tuning the operating regime of UE-side PDCCH detection in the activity–latency trade-off plane with a very fine granularity. Driven by economics and sustainability goals, the importance of DRX and other energy-saving features will only grow on the path toward 6G, and fine-tuning its operating point can maximize such savings. In addition, ML-aided policies, while remaining standard compliant, also have the potential to optimize DRX by leveraging other contextual data, such as scheduling decisions, traffic statistics, and obscure cross-UE interdependencies. Designing control policies capable of digesting such vast amounts of data in real-time is challenging. The simulation results presented in

⁴This relatively short cycle is chosen to align with the extremely low Packet Delay Budget (PDB) of XR traffic.

this paper suggest that automated policy discovery methods like the one described here are a fast and cost-effective way to achieve energy savings in 5G and beyond.

REFERENCES

- [1] A. Valcarce and J. Hoydis, "Toward joint learning of optimal MAC signaling and wireless channel access," *IEEE Transactions on Cognitive Communications and Networking*, vol. 7, no. 4, pp. 1233–1243, 2021.
- [2] E. Dahlman, S. Parkvall, and J. Sköld, *5G/5G-Advanced. The new generation wireless access technology (3rd ed.)*. Elsevier Ltd, 2024.
- [3] Y.-N. R. Li, M. Chen, J. Xu, L. Tian, and K. Huang, "Power saving techniques for 5G and beyond," *IEEE Access*, vol. 8, pp. 108 675–108 690, 2020.
- [4] Z. Corporation, "Consideration on UE power consumption model and preliminary evaluation results," Nov 2018. [Online]. Available: <https://portal.3gpp.org/ngppapp/TdocList.aspx?meetingId=18807>
- [5] 3GPP, "TS 38.321 NR Medium Access Control (MAC) protocol specification," 3rd Generation Partnership Project (3GPP), Technical Specification (TS), TSG-RAN1#48 R1-070674.
- [6] A. A. Esswie, "Power saving techniques in 3gpp 5g new radio: A comprehensive latency and reliability analysis," in *2022 IEEE Wireless Communications and Networking Conference (WCNC)*, 2022, pp. 66–71.
- [7] M. Memon, M. Maheshwari, D. Shin, A. Roy, and N. Saxena, "Deep-DRX: A framework for deep learning-based discontinuous reception in 5G wireless networks," *Transactions on Emerging Telecommunications Technologies*, vol. 30, 03 2019.
- [8] J. Zhou, G. Feng, T. S. P. Yum, M. Yan, and S. Qin, "Online learning-based discontinuous reception (DRX) for machine-type communications," *IEEE Internet of Things Journal*, vol. 6, no. 3, pp. 5550–5561, 2019.
- [9] P. Bruhn and G. Bassi, "Machine learning based C-DRX configuration optimization for 5G," in *Mobile Communication - Technologies and Applications; 25th ITG-Symposium*, 2021, pp. 1–6.
- [10] I. Akyildiz and H. Guo, "Wireless communication research challenges for Extended Reality (XR)," *ITU Journal on Future and Evolving Technologies (ITU J-FET)*, vol. 3, 04 2022.
- [11] V. Petrov, M. Gapeyenko, S. Paris, A. Marcano, and K. I. Pedersen, "Standardization of Extended Reality (XR) over 5G and 5G-Advanced 3GPP New Radio," 2022. [Online]. Available: <https://arxiv.org/abs/2203.02242>
- [12] A. Kuhne and A. Klein, "Throughput analysis of multi-user OFDMA-systems using imperfect CQI feedback and diversity techniques," *IEEE Journal on Selected Areas in Communications*, vol. 26, no. 8, pp. 1440–1450, 2008.
- [13] V. Mnih, K. Kavukcuoglu, D. Silver, A. Graves, I. Antonoglou, D. Wierstra, and M. A. Riedmiller, "Playing Atari with deep reinforcement learning," *CoRR*, vol. abs/1312.5602, 2013. [Online]. Available: <http://arxiv.org/abs/1312.5602>

Adriano Pastore, (Senior Member, IEEE) is a Senior Researcher at the Centre Tecnològic de Telecomunicacions de Catalunya, within the Research Unit on Information and Signal Processing for Intelligent Communications. He received a Diplôme de l'École Centrale Paris (now CentraleSupélec) in 2006 and a Dipl.-Ing. degree in electrical engineering in 2009 from the Technical University of Munich, and obtained his PhD from the Universitat Politècnica de Catalunya in 2014. From 2014 to 2016 he has been a postdoctoral researcher at École Polytechnique Fédérale de Lausanne (EPFL) with Prof. Michael Gastpar.

His topics of interest lie mainly in the fields of information theory and signal processing for wireless communications, machine learning for communications, physical-layer network coding, protocol learning, quantum key distribution, and privacy–utility tradeoffs.

Adrián Agustín, (Senior Member, IEEE) is a Senior Researcher at the Centre Tecnològic de Telecomunicacions de Catalunya (CTTC), within the Research Unit on Information and Signal Processing for Intelligent Communications (ISPIC). He received the M.S. and Ph.D in Telecommunication from Universitat Politècnica de Catalunya (UPC), Barcelona, Spain in 2000 and 2008, respectively. From 2008 to 2019 he was a research associate at the SPCOM group at UPC working in the different research areas of wireless communications. In April, 2021 he joined the CTTC.

He is interested in different research areas for developing next generation wireless communications at L1, L2, in particular with : Extremely Large Antenna Arrays (ELAA), Deep-Reinforcement Learning (DRL) and Random Access Networks.

Álvaro Valcarce, (Senior Member, IEEE) is Head of Department on Wireless AI/ML at Nokia Bell Labs, France. His research is focused on the application of machine learning techniques to L2 and L3 wireless problems for the development of technologies beyond 5G. He is especially interested on the potential of multiagent reinforcement learning for emerging novel L2 signaling protocols, as well as on the usage of Bayesian optimization for RRM problems. His background is on cellular networks, computational electromagnetics, optimization algorithms, and machine learning.